Available online at www.sciencedirect.com
ScienceDirect
Journal of Power Sources 159 (2006) 1389–1394
JOURNAL OF POWER SOURCES
www.elsevier.com/locate/jpowsour

Short communication

EPR studies of Li deintercalation from $LiCoMnO_4$ spinel-type electrode active material

Ekaterina Zhecheva [a,*], Radostina Stoyanova [a], Ricardo Alcántara [b], Pedro Lavela [b], José L. Tirado [b]

[a] *Institute of General and Inorganic Chemistry, Bulgarian Academy of Sciences, 1113 Sofia, Bulgaria*
[b] *Laboratorio de Química Inorgánica, Universidad de Córdoba, Edificio C-3, Primera Planta, Campus de Rabanales, 14071 Córdoba, Spain*

Received 27 June 2005; received in revised form 21 September 2005; accepted 25 November 2005
Available online 9 January 2006

Abstract

The electrochemical extraction/insertion of Li from/into $LiCoMnO_4$ in the potential range of 3.7–5.25 V is studied by electron paramagnetic resonance (EPR) of Mn^{4+}. Structural characterization of initial $LiCoMnO_4$ has been performed by neutron diffraction. The EPR spectra are consistent with a single-phase mechanism of electrochemical extraction/insertion of Li from/into $LiCoMnO_4$. During Li extraction, the intensity of the main EPR signal due to Mn^{4+} ions in Mn^{4+}/Co^{3+} environment decreases drastically concomitantly with the appearance of resonance absorption from magnetically correlated Mn^{4+}–Co^{4+} spins. From EPR, the complex [Co^{n+}–Mn^{3+}–Mn^{4+}] clusters indicative of the oxygen non-stoichiometry of $LiCoMnO_4$ also take part in the electrochemical reaction, especially up to 4.7 V. During the Li reinsertion, the EPR signal from Mn^{4+} ions in Mn^{4+}/Co^{3+} environment is recovered, but its intensity remains lower (30%) as compared to that of the initial composition, which is consistent with an unrecovered composition of $LiCoMnO_4$ electrode after first charge/discharge. Contrary to the narrow main signal, there is a reverse reduction of the paramagnetic ions present in the clusters, but their oxidation state as compared to the initial composition is not recovered.

Keywords: Cathode materials; Lithium cobalt–manganese spinel oxides; EPR spectroscopy; Structural characterisation; Lithium-ion batteries

1. Introduction

Among the most promising new positive electrodes for future lithium-ion batteries, $LiMPO_4$ compounds [1], manganese-based layered-type compounds [2,3] and manganese-based spinel-type compounds [4] can be cited. In the case of the manganese-based spinels, which can be considered as derived from $LiMn_2O_4$, a work voltage as high as ca. 5 V versus Li^+/Li can be achieved with partial manganese substitution by transition metals such as nickel [5–7], cobalt [8,9], iron [10] or combination of several of these elements [11–13]. A constant voltage region or plateau is developed at ca. 4.7 V versus Li^+/Li in the case of the extraction/insertion of lithium from/into $LiNi_{0.5}Mn_{1.5}O_4$, simultaneously to the occurrence of several cubic phases with different cell parameters, as was observed by using XRD [14,15]. In contrast, lithium extraction from the cobalt-containing manganese-based spinels takes place through a single-phase mechanism and then a plateau is not observed in the voltage–composition curve [11,12].

In order to maintain the electroneutrality, the composition limit for the $LiCo_xMn_{2-x}O_4$ solid solutions is $LiCoMnO_4$. The structure of manganese-based spinel-type compounds has been widely studied by using X-ray (XRD) and neutron (ND) diffraction experiments [4,16]. Thus, Strobel et al. using ND data previously reported the structure of $LiCo_{0.5}Mn_{1.5}O_4$, and a spinel-type structure corresponding to *Fd3m* space group was established [17]. XRD data for $LiCoMnO_4$ were reported by Kawai et al. [8]. Complimentary to the XRD techniques, spectroscopic methods (such us NMR and EPR) appear to be effective for studying the local cationic environment [18,19]. EPR has been successfully used for studying the cationic distribution in magnetically concentrated lithium–manganese spinels [20–26]. The replacement of Mn^{3+} in $Li_{1+x}Mn_{2-x}O_4$ by low-spin diamagnetic Co^{3+} ions yields solids spinel solutions

* Corresponding author. Tel.: +359 2 979 3915; fax: +359 2 870 50 24.
E-mail address: zhecheva@svr.igic.bas.bg (E. Zhecheva).

0378-7753/$ – see front matter © 2005 Elsevier B.V. All rights reserved.
doi:10.1016/j.jpowsour.2005.11.088

containing Mn^{4+} only (possessing a half-integer spin $S = 3/2$) [27], which are are especially suitable for EPR spectroscopy study at conventional microwave frequencies (9.3 GHz, X-band). Depending on the synthesis conditions, EPR spectra of Li[CoMn]O_4 compositions permit differentiation between samples in respect of the diamagnetic Co^{3+} and paramagnetic Mn^{4+} neighbors around Mn^{4+} [25,28]. In addition, for slightly non-stoichiometric $LiCoMnO_{4-\delta}$ oxides, an additional broad signal with $g > 2.2$ has been detected and attributed to [Co^{n+}–Mn^{3+}–Mn^{4+}] clusters, which are located in the lattice defect sites (such as, for example, oxygen defects). The observation of the EPR signals enables us to explore the electronic structure of $LiCoMnO_4$ during Li deintercalation/intercalation.

In this work, the oxidized/reduced $LiCoMnO_4$ electrodes are studied by using EPR. Neutron diffraction data of $LiCoMnO_4$ are reported here.

2. Experimental

A sample of $LiCoMnO_4$ nominal composition was prepared as follows. Firstly, LiOH, $Co(NO_3)_2$ and $Mn(NO_3)_2$ were added to water with continuous stirring, and heating until dryness. The resulting powder was manually ground in an agate mortar and heated to 400 °C and annealed in air atmosphere for 1 day. After grinding, the obtained solid was further heated to 800 °C, annealed for 3 days in air atmosphere, ground, further annealed at 800 °C during 3 days, ground again, re-annealed at 600 °C during 3 days and quenched from this temperature. The room temperature neutron diffraction experiments were carried out at the Institute Laue-Langevin (Grenoble, France) using a D1A instrument ($\lambda = 1.9114$ Å), 0.1°-steps and 4 h of recording for each sample. Rietveld refinement was carried out using the WinplotR-Fullprof programs [29].

The electrochemical oxidation of $LiCoMnO_4$ was carried out by using two-electrode Swagelok™ cells of the type Li|$LiPF_6$(EC:DEC)|$LiCoMnO_4$. The positive electrodes contained about 10 mg cm^{-2} of active material (86% of the composite), 6% of PVDF binder, and 8% of carbon (50% weight mixture of graphite and carbon black), supported onto an aluminum foil, cut as a 9 mm diameter disk, dried at 120 °C under vacuum and pressed. Lithium electrodes consisted of a clean 9 mm diameter lithium metal disk. The electrolyte solution was a commercial (Merck LP40) 1 M $LiPF_6$ solution in a 1:1 (w/w) mixture of ethylene carbonate (EC) and diethyl carbonate (DEC), which was supported by porous Whatman™ glass-paper discs that also served as separators. The electrochemical oxidation was carried out by galvanostatic charge using a multichannel MacPile II system, at *C*/10 rate, i.e. one Li extracted from $LiCoMnO_4$ in 10 h.

The EPR spectra were recorded as a first derivative of the absorption signal of an ERS-220/Q (ex-GDR) spectrometer within the temperature range of 100–300 K. The *g*-factors were determined with respect to a Mn^{2+}/ZnS standard. The signal intensity was established by double integration of the experimental EPR spectrum. To obtain the ex situ EPR spectra of the electrochemically oxidized (charge process) $LiCoMnO_4$, the electrochemical process was interrupted at selected charge levels and then, after a relaxation period the electrochemical cells were dismounted in a dry-box and the electrodes were recuperated.

3. Results and discussion

The ND pattern of the studied $LiCoMnO_4$ sample and the corresponding Rietveld simulation are shown in Fig. 1. Superstructure reflections are not observed, in contrast with ordered $LiNi_{0.5}Mn_{1.5}O_4$ [17,30]. The structural results obtained by using the Rietveld refinement are shown in Table 1. The best fitting was obtained by using a three-phase model. The main phase was $LiCoMnO_4$ with Co_3O_4 and Li_2MnO_3 as minor phases. Although we tested different preparation conditions (from 600 to 950 °C annealing temperature) all ours essays to obtain a single-phase sample were unsuccessful. The detection of impurities is consistent with previous studies [31]. For the spinel-type compound with $LiNi_{0.5}Mn_{1.5}O_4$ nominal composition, which corresponds to the electroneutrality limit of composition in the $LiNi_xMn_{2-x}O_4$ solid solutions, minor impurities are also frequently observed [5,17]. The main phase $LiCoMnO_4$ is a normal spinel, in which Li occupies tetrahedral 8a sites and Co/Mn are located in octahedral 16d sites (Table 1). The occurrence of Li in the 16d sites and/or Co/Mn in the 8a sites was tested with the Rietveld refinement, and then this possibility was discarded.

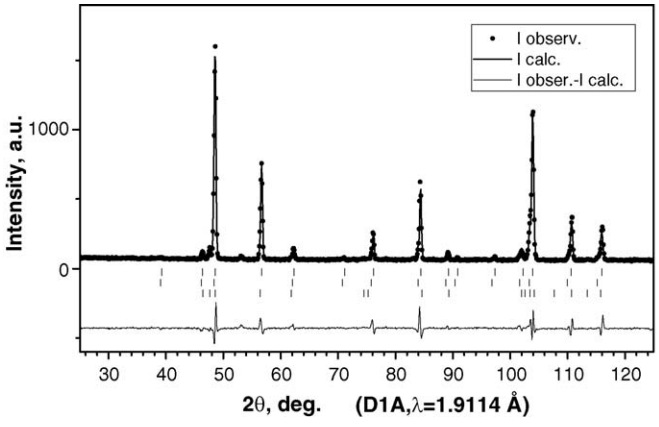

Fig. 1. Observed (points) and calculated neutron diffraction pattern and different between them for $LiCoMnO_4$ sample.

Table 1
Summary of Rietveld refinements results of neutron diffraction data on $LiCoMnO_4$

Global refinement parameters	Spinel phase results						
R_{Bragg}	χ^2	Space group	Cell parameter (Å)	*z* (O)	R_f	R_{Bragg}	Structural formula[a]
5.27	7.53	*Fd3m*	8.0506	0.2632	2.93	2.94	$(Li)_{tet}[CoMn]_{oct}O_4 + 7.2\%\ Co_3O_4 + 15.1\%\ Li_2MnO_3$

[a] Mass fraction of foreign phases from Rietveld refinement.

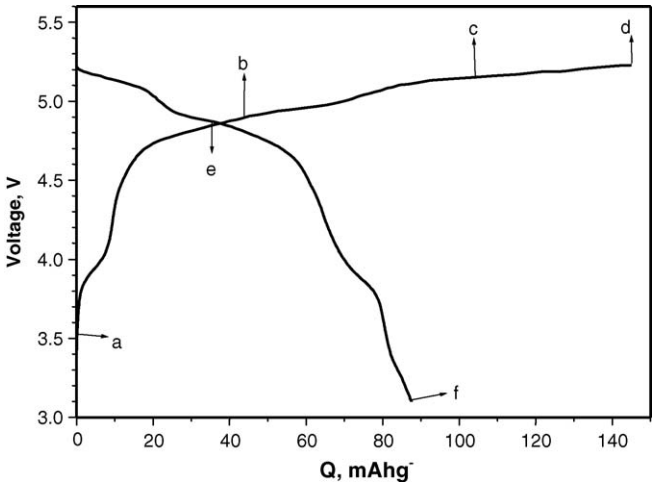

Fig. 2. Voltage vs. capacity curves corresponding to charge and discharge of $LiCoMnO_4$ in lithium cell. The points in which the electrochemical experiments were interrupted to register the EPR spectra have been marked (a–f).

The structural model for $LiCoMnO_4$ that can be deduced from ND results is in good agreement with the previously reported XRD data [9,11].

The electrochemical charge/discharge cycle of $LiCoMnO_4$ in the lithium cell is shown in Fig. 2. The extraction, and insertion, of lithium from $LiCoMnO_4$ takes place mostly between 4.5 and 5.2 V versus Li^+/Li. There is also a short voltage region at about 4.0 V, which is smaller than 10 mAh g^{-1} and that is indicative of the Mn^{3+}/Mn^{4+} redox couple. The 4-V capacity is indicative of a slight oxygen deficiency, which is in line with the EPR results. The capacity of the consequent discharge is lower than the capacity of the previous charge (Fig. 2), indicating the occurrence of irreversible processes, such undesirable reactions with the electrolyte [11,32]. The EPR experiments of charged and charged/discharged $LiCoMnO_4$-electrodes were carried out in the selected points, which are marked 'a–f' in Fig. 2. During the first charge, assuming that there are no parallel reactions and that all the electrons are used for lithium extraction from $LiCoMnO_4$, these points correspond to the following formulae: (a) $LiCoMnO_4$, (b) $Li_{0.7}CoMnO_4$—30% of lithium extraction, (c) $Li_{0.3}CoMnO_4$—70% of lithium extraction and (d) Li_0CoMnO_4—100% of lithium extraction. Selected points after completed first charge and consequent partial discharge to $Li_{0.25}CoMnO_4$ nominal composition (e) and complete discharge (f) were also studied.

Fig. 3 compares the EPR spectrum at 213 K of initial $LiCoMnO_4$ with EPR spectra of electrochemically delithiated and relithiated $LiCoMnO_4$. In accordance with previous EPR data on $LiCoMnO_4$ [28], the EPR spectrum of $LiCoMnO_4$ displays two overlapping signals characterized by different g-factors and line widths. The main signal (the narrower one) ascribable to antiferromagnetically coupled Mn^{4+} ions in Co^{3+}, Mn^{4+}-environment, possesses a Lorentzian line shape, a g-factor of 2.004 and a line width width, which increases with the decrease in the recording temperature (Fig. 4). The Lorentzian line shape is also used to fit the additional broader signal. For this signal, the effective g-factor decreases and the line width

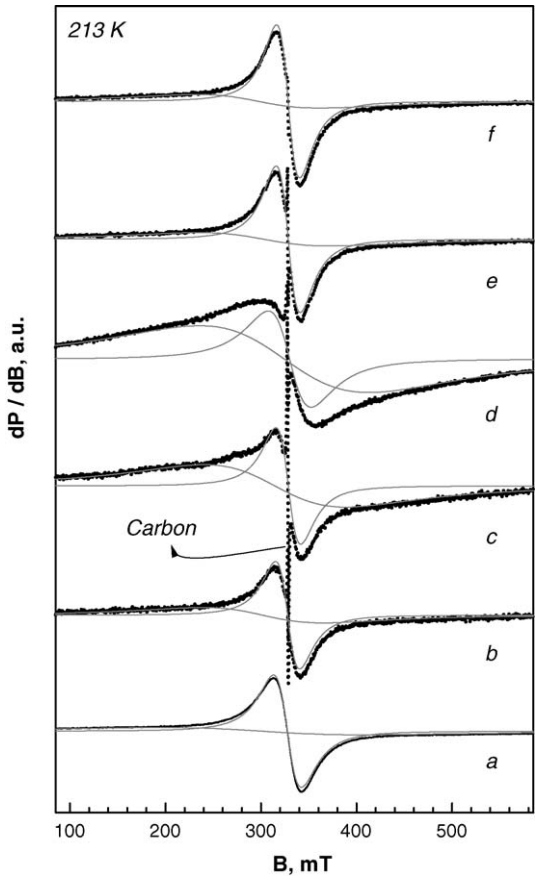

Fig. 3. EPR spectra of $LiCoMnO_4$ after Li extraction of 0% (a), 30% (b), 70% (c), 100% (d) and consecutive Li insertion of 50% (e) and 100% (f).

increases when the recording temperature decreases. Based on the previous EPR studies of $LiCo_xMn_{2-x}O_4$, the appearance of the broader signal has been related to slight non-stoichiometry of $LiCoMnO_4$, where complex $[Co^{n+}–Mn^{3+}–Mn^{4+}]$ clusters are formed [28].

During partial Li deintercalation from $LiCoMnO_4$, the EPR spectrum still displays two overlapping signals (Fig. 3). Between 293 and 143 K, the line width of the main signal due to Mn^{4+} ions remains unchanged during Li extraction up to 70%, while a slight decrease in the g-factor is observed (Table 2). However, the EPR intensity of this signal is drastically reduced during Li extraction: from $I = 1.0$ for the initial sample to $I = 0.2$ and 0.05 after extraction of 30 and 70% lithium, respectively. On the other hand, in the same Li concentration range there is a decrease in the effective g-factor and the line width for the broader signal from the $[Co^{n+}–Mn^{3+}–Mn^{4+}]$ clusters (Table 2). An important difference between the initial and the delithiated compositions is the temperature insensitivity of the effective g-factor of the broader signals in the temperature range of 293–143 K (Table 2). Moreover, the value of the effective g-factor decreases as the amount of the extracted Li increases: $g = 2.16$, 2.09 and 2.02 for the composition with 30, 70 and 100% extracted Li, respectively (Table 2). These results indicate oxidation of the Mn^{3+} ions in the $[Co^{n+}–Mn^{3+}–Mn^{4+}]$-clusters to Mn^{4+} ions mainly. It appears that the Mn^{4+} ions become the only paramagnetic ions in these clusters during Li deintercalation. In addition, resonance absorp-

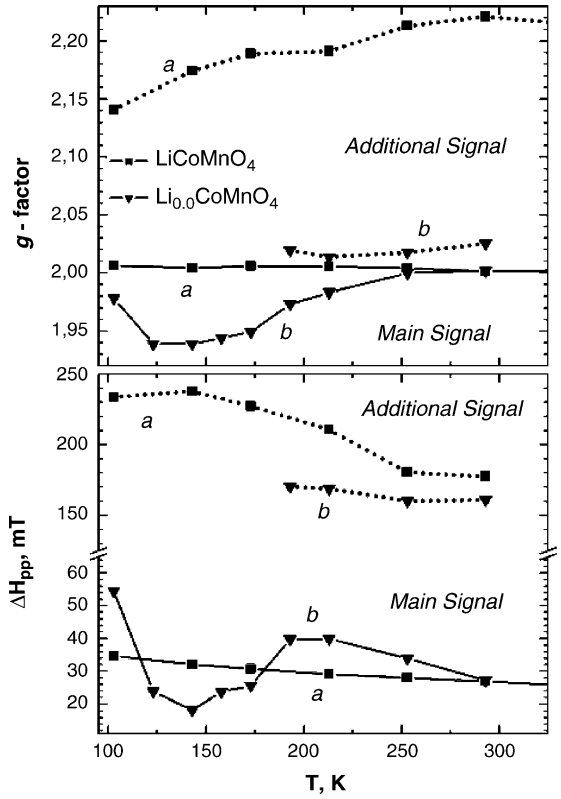

Fig. 4. Temperature variation of the g-factor and the line width (ΔH_{pp}) for the signal due to Mn^{4+} in Co^{3+}, Mn^{4+}-environment (full lines) and the additional broader signals due to the complex [Co^{n+}–Mn^{3+}–Mn^{4+}] clusters (dotted lines) detected for initial $LiCoMnO_4$ (a) and $LiCoMnO_4$ after 100% of Li extraction (b).

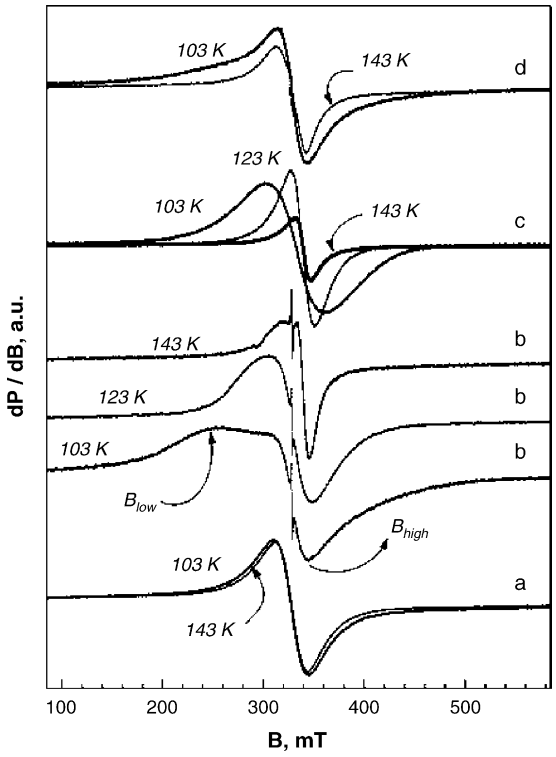

Fig. 5. EPR spectra of $LiCoMnO_4$ after lithium extraction of 0% (a), 30% (b), 100% (c) and after 100% Li reinsertion (d). The absorption in low- and high-magnetic field is indicated.

tion in the low- and high-magnetic field appears below 143 K, the positions being sensitive to the recording temperature (Fig. 5). This means that below 150 K an EPR response from magnetically correlated spins is detected instead of the high-temperature EPR signal due to localized paramagnetic centers. However, no long-range magnetic order is achieved in this temperature range.

For fully delithiated oxides, two overlapping signals can also be resolved between 293 and 193 K. Below 193 K, only one signal is detected (Fig. 5). This signal is different in comparison with the main signal observed for the initial composition. For the fully delithiated composition, the g-factor of the signal displays dependence on the recording temperature (Fig. 4). The line width decreases from 193 to 143 K, followed by a line broadening below 140 K. It is important to note that, between 100 and 290 K, the Lorentzian line shape fits well the profile of the EPR signals (Figs. 3 and 5). The temperature dependence of the g-factor indicates an appearance of alien paramagnetic ions in the vicinity of Mn^{4+} ions, but magnetically correlated spins are not observed.

The consecutive Li insertion restores the EPR parameters of the narrow signal (Fig. 3; Table 2). However, an EPR response from magnetically correlated is still visible below 143 K. In addition, the broader signal remains different as compared to that of the initial composition. The effective g-factor is still insensitive to the recording temperature and the line width is lower with respect to the initial composition (Table 2).

To rationalize the observed changes in the EPR spectra of delithiated and relithiated $LiCoMnO_4$, the metal oxy/redoxy pairs involved in the electrochemical reaction at 5 V can be taken into account. The electrochemical extraction of Li proceeds together with the oxidation of Co^{3+} to Co^{4+}, while Mn^{4+} remains electrochemically inactive. However, the Mn^{4+} ions

Table 2
EPR line width (ΔH_{pp}) and g-factor of the main signal due to Mn^{4+} in Mn^{4+}, Co^{3+}-environment and the broader additional signal due to [Co^{n+}–Mn^{3+}–Mn^{4+}] clusters

Compounds	EPR signal due to Mn^{4+} in Mn^{4+}, Co^{3+}-environment		EPR signal due to [Co^{n+}–Mn^{3+}–Mn^{4+}] clusters		
	ΔH_{pp}, mT (213 K)	g-Factor (213 K)	ΔH_{pp}, mT (213 K)	g-Factor (213 K)	g-Factor (293 K)
$LiCoMnO_4$	29.2	2.005	210.7	2.191	2.221
First charge—30% of extracted Li	25.0	2.002	125.6	2.161	2.174
First charge—70% of extracted Li	26.1	2.000	148.5	2.090	2.103
First charge—100% of extracted Li	39.9	1.983	168.5	2.014	2.0252
First discharge—50% of reinserted Li	25.3	2.000	137.1	2.167	2.177
First discharge—100% of reinserted Li	24.3	2.002	127.9	2.214	2.217

are the only paramagnetic species registered by X-band EPR. Contrary to diamagnetic Co^{3+}, the electrochemically generated Co^{4+} is paramagnetic (d^5 configuration). In X-band EPR experiments, low-spin Co^{4+} ions usually remain EPR silent due to the high magnitude of the zero field splitting parameter. However, the appearance of alien paramagnetic Co^{4+} ions near Mn^{4+} will be responsible for the change in EPR behavior of the delithiated $Li_{1-x}CoMnO_4$. Since there are no data on the magnetic structure of spinels containing paramagnetic Co^{4+} and Mn^{4+} in 16d sites simultaneously, it is worth mentioning the EPR response from Mn^{4+} and Ni^{2+} containing spinels such as $LiMg_{0.5-x}Ni_xMn_{1.5}O_4$ where paramagnetic Ni^{2+} replaces diamagnetic Mg^{2+}. Passing from Mg^{2+}- to Ni^{2+}-substituted spinels, the magnetic structure changes from ferromagnetic to ferrimagnetic at a Currie temperature of 38 and 130 K, respectively [32–34]. Whereas above 40 K localised Mn^{4+} ions cause the appearance of a single Lorentzian line in the EPR spectrum of $LiMg_{0.5}Mn_{1.5}O_4$, for $LiNi_{0.5}Mn_{1.5}O_4$ an EPR response from residual antiferromagnetically correlated Ni^{2+}–Mn^{4+} spins is detected between 140 and 413 K [30]. For the fully delithiated $Li_{1-x}CoMnO_4$ composition ($x \rightarrow 1$), which contains simultaneously paramagnetic Co^{4+} and Mn^{4+} in 16d spinel sites, one can expect to observe an EPR response from magnetically correlated spins of alien Co^{4+} and Mn^{4+}, and resonance field and line width will be dependent on the recording temperature. This is what we observe for the narrow signal for fully delithiated $Li_{1-x}CoMnO_4$: the effective g-factor and the line width display complex temperature dependence between 100 and 290 K (Fig. 4).

The effect of paramagnetic Co^{4+} on the EPR spectrum of Mn^{4+} can also be related to the appearance of the low- and high-field resonance absorption below 143 K for partially delithiated and relithiated spinels. For partially delithiated oxides, the detection of the narrow signal due to Mn^{4+} surrounded by Co^{3+} and Mn^{4+} shows that the local environment of Mn^{4+} is preserved. Of importance is that its intensity is drastically reduced during lithium extraction. It appears that after extraction of 30% Li (up to 4.7 V), the content of electrochemically generated Co^{4+} ions is sufficient to cause the development of magnetic interactions in a macro-scale range. Since the electrochemical extraction of Li proceeds by a single-phase mechanism [11,12], the EPR result indicates that some $LiCoMnO_4$ particles do not take part in the electrochemical reaction: even after 70% of lithium extraction, about 5% of the $LiCoMnO_4$ particles remain inactive. To improve the electrochemical performance of $LiCoMnO_4$, it is of importance to understand the reason for incomplete participation of $LiCoMnO_4$ particles in the electrochemical reaction.

After Li reinsertion, the EPR parameters of the narrow signal are recovered, but the signal intensity remains lower (30%) as compared to that of the initial composition. This is in good accordance with the unrecovered composition of the $LiCoMnO_4$ electrode determined from electrochemical charge/discharge processes (Fig. 2).

The third feature of the EPR spectra of delithiated and relithiated oxides is associated with the broader signal, which is suggested to correspond to complex [Co^{n+}–Mn^{3+}–Mn^{4+}] clusters. The strong changes in both the effective g-factor and the line width reveal, on the one hand, that these clusters are electrochemically active especially at the beginning of the electrochemical reaction (between 3.8 and 4.7 V). This is consistent with the fact that Mn^{3+} in 16d spinel sites is oxidised to Mn^{4+} in the 4 V-region, where Co^{3+} is electrochemically inactive. On the other hand, the smooth decrease in value of the effective g-factor implies progressive changes in the oxidation state of Co and/or Mn. After Li reinsertion, there is a back reduction of the paramagnetic ions included in the clusters, but their oxidation state, as compared to the initial composition, is not recovered.

4. Conclusions

According to neutron diffraction results, the $(Li)_{tet}[CoMn]_{oct}O_4$ normal spinel crystallizes in a structure corresponding to the *Fd3m* space group. Superstructure reflections are not observed. Mn^{4+} ions in octahedral spinel sites account for the appearance of an EPR signal with Lorentzian line shape and $g = 2.004$. The slight non-stoichiometry of $LiCoMnO_4$ is responsible for the appearance of a broader signal attributed to complex [Co^{n+}–Mn^{3+}–Mn^{4+}] clusters. The electrochemical extraction/insertion of Li from/into $LiCoMnO_4$ proceeds by a single-phase mechanism. After electrochemical Li extraction, the intensity of the main signal decreases drastically concomitantly with the appearance of resonance absorption due to magnetically correlated Mn^{4+}–Co^{4+} spins. The complex [Co^{n+}–Mn^{3+}–Mn^{4+}] clusters take also part in the electrochemical reaction, especially up to 4.7 V. During the Li reinsertion, the EPR parameters of the main signal are recovered, but the signal intensity remains lower (30%) as compared to that of the initial composition. This is in good accordance with the unrecovered composition of the $LiCoMnO_4$ electrode after the first charge/discharge. Contrary to the narrow main signal, there is a reverse reduction of the paramagnetic ions included in the clusters, but their oxidation state as compared to the initial composition is not recovered.

Acknowledgments

Authors are indebted to the Institute Laue-Langevin (Grenoble) for the use of the neutron diffraction facilities, and also thank the financial support from MEC (Programa Ramón y Cajal and contract MAT2002-00434). E.Zh. and R.S. greatly appreciate the support of the National Science Fund of Bulgaria (Contract no. Ch1304/2003).

References

[1] X.A. Huang, J.F. Ma, P.W. Wu, Y.M. Hu, J.H. Dai, Z.B. Zhu, H.Y. Chen, H.F. Wang, Mater. Lett. 59 (2005) 578.
[2] C.S. Johnson, J.S. Kim, A.J. Kropf, A.J. Kahaian, J.T. Vaughey, L.M.L. Fransson, K. Edström, M.M. Thackeray, Chem. Mater. 15 (2005) 2313.
[3] R. Stoyanova, E. Zhecheva, L. Zarkova, Solid State Ionics 73 (1994) 233.
[4] M.M. Thackeray, Prog. Solid State Chem. 25 (1997) 1.
[5] Q. Zhong, A. Bonakdarpour, M. Zhang, Y. Gao, J.R. Dahn, J. Electrochem. Soc. 144 (1997) 205.
[6] T. Ohzuku, K. Ariyoshi, S. Yamamoto, Y. Makimura, Chem. Lett. (2001) 1270.
[7] R. Alcántara, M. Jaraba, P. Lavela, J.L. Tirado, P. Biensan, A. de Guibert, C. Jordy, J.P. Peres, Chem. Mater. 15 (2003) 2376.

[8] H. Kawai, M. Nagata, H. Tukamoto, A.R. West, Electrochem, Solid State Lett. 1 (1998) 212.
[9] H. Kawai, M. Nagata, H. Tukamoto, A.R. West, J. Power Sources 81–82 (1999) 67.
[10] T. Ohzuku, K. Ariyoshi, S. Takeda, Y. Sakai, Electrochim. Acta 46 (2001) 2327.
[11] R. Alcantara, M. Jaraba, P. Lavela, J.L. Tirado, Chem. Mater. 15 (2003) 1210.
[12] R. Alcántara, M. Jaraba, P. Lavela, J.L. Tirado, J. Electrochem. Soc. 151 (2004) A53.
[13] R. Alcántara, M. Jaraba, P. Lavela, J.M. Lloris, C.P. Vicente, J.L. Tirado, J. Electrochem. Soc. 152 (2005) A13.
[14] R. Alcántara, M. Jaraba, P. Lavela, J.L. Tirado, Electrochim. Acta 47 (2002) 1829.
[15] K. Ariyoshi, Y. Iwakoshi, N. Nakayama, T. Ohzuku, J. Electrochem. Soc. 151 (2004) A296.
[16] P. Strobel, F. Le Cras, L. Seguin, M. Anne, J.M. Tarascon, J. Solid State Chem. 135 (1998) 132.
[17] P. Strobel, A. Ibarra-Palos, M. Anne, C. Poinsignon, A. Crisci, Solid State Sci. 5 (2003) 1009.
[18] C.P. Grey, N. Dupre, Chem. Rev. 104 (2004) 4493.
[19] E. Zhecheva, R. Stoyanova, R. Alcántara, P. Lavela, J.L. Tirado, Pure Appl. Chem. 74 (2002) 1885.
[20] V. Massarotti, D. Capsoni, M. Bini, C.B. Azzoni, J. Solid State Chem. 128 (1997) 80.
[21] R. Stoyanova, M. Gorova, E. Zhecheva, J. Phys. Chem. Solids 61 (2000) 609.
[22] D. Capsoni, M. Bini, G. Chiodelli, V. Massarotti, M.C. Mozatti, A. Comin, Phys. Chem. Chem. Phys. 3 (2001) 2162.
[23] D. Capsoni, M. Bini, G. Chiodelli, P. Mustarelli, V. Massarotti, C. Azzoni, M.C. Mozatti, L. Linati, J. Phys. Chem. B 106 (2002) 7432.
[24] D. Capsoni, M. Bini, G. Chiodelli, V. Massarotti, M.C. Mozatti, C. Azzoni, Solid State Commun. 125 (2003) 179.
[25] E. Zhecheva, R. Stoyanova, M. Gorova, P. Lavela, J.L. Tirado, Solid State Ionics 140 (2001) 19.
[26] S. Mandal, R.M. Rojas, J.M. Amarilla, P. Calle, N.V. Kosova, V.F. Anufrienko, J.M. Rojo, Chem. Mater. 14 (2002) 1598.
[27] S. Suzuki, M. Tomita, S. Okada, H. Arai, J. Phys. Chem. Solids 57 (1996) 1851.
[28] R. Stoyanova, E. Zhecheva, M. Gorova, J. Mater. Chem. 10 (2000) 1377.
[29] Rodríguez-Carvajal, Physica B 192 (1995) 55.
[30] R. Alcántara, M. Jaraba, P. Lavela, J.L. Tirado, E. Zhecheva, R. Stoyanova, Chem. Mater. 16 (2004) 1573.
[31] A.R. West, H. Kawai, H. Kageyama, M. Tabuchi, M. Nagata, H. Tukamoto, J. Mater. Chem. 11 (2001) 1662.
[32] R. Alcántara, M. Jaraba, P. Lavela, J.L. Tirado, J.C. Jumas, J. Olivier Fourcade, J. Power Sources 135 (2004) 281.
[33] G. Blasse, J. Phys. Chem. Solids 27 (1966) 383.
[34] W. Branford, M.A. Green, D.A. Neumann, Chem. Mater. 14 (2002) 1649.